

PS

Confinement and the Safety Factor Profile

S. H. Batha and F. M. Levinton

Fusion Physics and Technology, Torrance, CA 90503

S. D. Scott, D. R. Mikkelsen, R. V. Budny, Z. Chang, H. Park,

E. Synakowski, G. Taylor, and M. C. Zarnstorff

Princeton Plasma Physics Laboratory, P.O. Box 451, Princeton, NJ 08543

S. A. Sabbagh

Department of Applied Physics, Columbia University, New York, New York 10027

(Received

The conjecture that the safety factor profile, $q(r)$, controls the improvement in tokamak plasmas from poor confinement in the Low- (L-) mode regime to improved confinement in the supershot regime has been tested in two experiments on the Tokamak Fusion Test Reactor (TFTR) [Plasma Phys. Controlled Nucl. Fusion Res. 1, 51 (1987)]. First, helium was puffed into the beam-heated phase of a supershot discharge which induced a degradation from supershot to L-mode confinement in about 100 msec, far less than the current relaxation time. The q and shear profiles measured by a motional Stark effect polarimeter showed little change during the confinement degradation. Second, rapid current ramps in supershot plasmas altered the q profile, but were observed not to change significantly the energy confinement. Thus, enhanced confinement in supershot plasmas is not due to a particular q profile which has enhanced stability or transport properties. The discharges making a continuous transition between supershot and L-mode confinement were also used to test the critical-electron-temperature-gradient transport model. It was found that this model could not reproduce the large changes in electron and ion temperature caused by the change in confinement.

PACS Numbers: 52.55.Pi, 52.25.Fi, 52.55.Fa

MASTER

1
DISTRIBUTION OF THIS DOCUMENT IS UNLIMITED *OT*

RECEIVED

MAR 13 1996

OSTI

DISCLAIMER

Portions of this document may be illegible in electronic image products. Images are produced from the best available original document.

I. Introduction

Several techniques have been developed to improve energy and particle confinement to more than double Low- (L-) mode values in a tokamak discharge. One example of importance is the supershot regime² on the Tokamak Fusion Test Reactor (TFTR),³ as well as on other tokamaks, which is reached by aggressive conditioning of the carbon limiter to reduce particle influx from the wall of the vacuum vessel.⁴ The supershot regime is of considerable practical importance since the highest values of energy confinement time, ion temperature, and reactivity triple product $n_e \tau_E T_i$ (electron density, energy confinement time and ion temperature, respectively) in DD discharges in TFTR have been reached in the supershot regime. Most of the DT phenomena being studied in TFTR have used this regime because it realizes a factor of 5 to 10 higher DT fusion rates and β_α , the β due to fusion-generated energetic alpha particles, than do L-mode plasmas.⁵

The supershot regime has four characteristics that distinguish it from the L-mode regime: (1) peaked electron density profiles, (2) high values of T_i and of the ratio T_i/T_e where T_e is the electron temperature (this ratio is about 1 in L-mode and about 3 in supershot plasmas), (3) low core ion thermal diffusivity, and (4) low edge influx of carbon and hydrogen.² The cause of the supershot enhanced confinement is of general interest because discharges having characteristics similar to supershots have been obtained on other tokamaks such as the Joint European Torus (JET),⁶ DIII-D,⁷ the Japan Atomic Energy Research Institute Tokamak-60 (JT-60U),⁸ and the Torus Experiment for Technological Oriented Research (TEXTOR).⁹ Such regimes have a variety of names such as "hot-ion mode" or "I-mode" confinement. A supershot plasma does not evolve from or make a transition from an L-mode plasma. The two types of discharges are fundamentally different in that the transport properties of the L-mode and supershot regimes are distinct, particularly the scaling with temperature and heating power,¹⁰ and so are a valuable test for transport models.

The supershot may be an attractive operational mode for a reactor since the peaked density and temperature profiles lead to high values of the figure of merit for neutron production $\beta^* \equiv 2\mu_0 \langle p^2 \rangle^{1/2} / B \text{Sup}5(2,t)$, where p is the pressure and B_t the toroidal field.⁵ An understanding of the physics mechanisms underlying the favorable properties of supershots could be used to improve the performance or to reduce the size of an ignited tokamak. However, supershots have not been used in the design of

future reactors such as the International Thermonuclear Experimental Reactor (ITER).¹¹ One reason is that it is not clear how to obtain the low particle influx in ITER that seems to be required for supershot operation.

The cause of the improved confinement of supershots is still under investigation. For example, it is not understood how a reduction in particle recycling at the plasma edge could improve core confinement. Experiments have shown that edge density perturbations generated by a helium gas puff caused the power flows and confinement to deteriorate in the core before they did further out in radius.¹² This occurred even though perturbations of local density and temperature propagated inward from the edge to the core.

Various hypotheses to explain the good confinement of supershots have been investigated. A strong correlation between the total stored energy and H_{ne} , the neutral-beam particle deposition shape factor, has been observed in L-mode and supershot discharges.¹³ However, the improvement in performance by a supershot is greater than that expected solely from a change in heating deposition assuming *constant* local values of the ion and electron thermal diffusivities, χ_i and χ_e , consistent with local transport analyses which show a marked reduction in χ_i between L-mode and supershot discharges.¹⁴ It has also been demonstrated that supershots are not controlled by marginal stability to ion-temperature-gradient-driven turbulence (ITGDT).^{15,16} However, more recent nonlinear gyrofluid simulations which predict the thermal transport of ITG modes¹⁷ have been found to be in qualitative agreement with the observed transport in supershots including the role of the edge conditions and how they affect core transport. Modeling calculations based on analytic representations of χ_i driven by ITG modes also qualitatively reproduce the L-mode to supershot differences.¹⁸

Supershot plasmas differ from L-mode plasmas in several ways that might be expected to affect the q (safety factor) and current profiles: They have a broader electron temperature profile, higher edge T_e , a larger contribution from bootstrap currents, and a larger Shafranov shift than L-mode plasmas. Therefore it is interesting to evaluate how supershot transport is affected by the q profile, and in particular whether the improved core confinement in supershots is caused by a modification from the q profile prevalent in L-mode plasmas. This hypothesis was tested in two ways. The first, described in section II, degraded a supershot discharge to L-mode confinement levels with a He gas puff. The main

result of this paper is a comparison of the q profiles measured by a motional-Stark-effect (MSE) polarimeter¹⁹⁻²¹ before and after the confinement-mode change. A second test of confinement sensitivity to the q profile was made by rapidly changing the total plasma current in a supershot which drastically changed the q profile. The result of this experiment is presented in section III. The q profile may affect the ultimate performance of a supershot by the action of magnetohydrodynamic (MHD) instabilities as discussed in section IV.

A proposed transport model, the critical-electron-temperature gradient model,¹¹ also known as the Rebut-Lallia-Watkins, RLW, or Rebut-Lallia-Watkins-Boucher model, has been shown to model JET discharges quantitatively.^{11,22-25} If this model also quantitatively models TFTR supershots, the underlying physical reasons for improved transport may be found in the assumptions of the model. Because this model assumes a strong dependence of the anomalous electron thermal diffusivity on the q profile as $\chi_{an,e} \propto q^2$, it is particularly appropriate to test the model with these plasmas. The applicability of this model to supershot discharges is important since the RLW formalism is being used to design the hardware and the operating scenarios of ITER.²⁶ The ability of the RLW model to predict the changes in electron and ion temperatures during the supershot to L-mode degradation is addressed in section V.

II. Confinement Variation

The supershot to L mode comparison was made by creating a typical TFTR supershot and spoiling the energy confinement with a He gas puff. Because helium is absorbed by the TFTR carbon limiter in about 1 sec which is comparable to the duration of a TFTR discharge,²⁷ the helium rapidly increases the edge neutral influx, reduces the edge ion temperature, and within one energy confinement time reproducibly produces plasmas with broad density profiles and greatly reduced ion energy confinement.¹²

Figure 1 shows the plasma parameters for the spoiled supershot and a companion supershot that was not spoiled. The discharges were created identically: The plasma current was 1.4 MA, the major radius of the last closed flux surface was 2.62 m, and the discharges were heated with 17.6 MW of balanced co- and counter-tangential neutral-beam power beginning at 3.7 sec. To spoil the discharge, approximately 14.5 torr-l of He was injected into the torus between 4.20 and 4.29 sec. At this time, the

q profile had almost fully relaxed to a steady-state value. As shown in Fig. 1, both discharges had identical stored energy, poloidal beta β_{pol} , and $q(0)$ before the gas puff. The central electron density, $n_e(0)$, and density peaking factor, $n_e(0)/\langle n_e \rangle$ (where $\langle n_e \rangle$ is the volume-averaged electron density), for the spoiled supershot were slightly higher before the gas puff due to He accumulated from intervening discharges. An identical response is observed in other experiments where there is no helium in the discharge before the gas puff. The energy confinement time enhancement over Goldston L-mode scaling,¹ $\tau_E/\tau_{E,L}$, was also the same for both discharges. At the beginning of the pulse, $\tau_E/\tau_{E,L} = 2.0$ and $n_e(0)/\langle n_e \rangle = 2.1$, which are typical values for a supershot plasma. The central ion temperature as measured by charge-exchange recombination spectroscopy²⁸ was the same, within the uncertainty of the measurement, before the gas puff. It is readily apparent in Fig. 1 that each of these parameters, except for $q(0)$, was degraded after the gas puff. For example, $\tau_E/\tau_{E,L}$ fell from 2 to less than 1.25 and the density peaking factor fell from 2.1 to 1.5.

The ion and electron temperature profiles from the spoiled supershot before and after the gas puff are shown in Figs. 2 and 3, respectively. The profiles at both times for the supershot without a gas puff are the same as the spoiled supershot before the gas puff, showing that the discharge had reached equilibrium before the gas was injected. The gas puff caused the ion temperature, Fig. 2, to decrease throughout the plasma, with the central temperature falling from 17 to 5 keV. The electron temperature, as measured by electron-cyclotron emission (ECE),²⁹ also decreased (Fig. 3), but by a lesser amount and the profile remained quite peaked. The electron density, measured by a 10-channel far infrared laser interferometer,³⁰ increased by about 25% in the center but doubled at the plasma edge and so became less peaked. The ion thermal diffusivity, χ_i , increased by an order of magnitude within $r < a/3$, but was unchanged at larger radius. Each profile after the gas puff had the characteristics of a usual L-mode plasma.

The internal magnetic field was measured using a MSE polarimeter.¹⁹⁻²¹ These measurements, in conjunction with external magnetic field measurements and the kinetic pressure profile, were used by the Variational Moments Equilibrium Code (VMEC)³¹ to determine the q , shear, and current profiles. The resulting q and shear profiles, as a function of the square root of the normalized toroidal flux, $X \equiv R(\Phi/\Phi(a))$, are shown in Figs. 4 and 5, respectively. The toroidal flux coordinate was chosen because

the lower stored energy in the L-mode phase caused the magnetic axis to move inwards, preventing direct comparisons in terms of major radius. On these graphs, the magnetic axis is at $X = 0$ while the edge of the plasma is at $X = 1$.

The unspoiled supershot showed little change in the q profile, Fig. 4, from 4.19 to 4.47 sec. The difference in $q(X)$ was less than 10%, with $q(0)$ having fallen slightly and the largest decrease occurring at $X = 0.75$. The changes in $q(X)$ for the spoiled supershot were similarly small. The largest change, by $\Delta q = -0.2$, was at $x = 0.70$. There was a modest increase in q at the edge of the plasma due to the change in the stored energy. All of the inferred changes are smaller than the estimated 10% uncertainty in the equilibrium reconstruction.³²

Profiles of the magnetic shear, defined as $s \equiv 2(V/q) (\partial q/\partial \psi) (\partial \psi/\partial V)$ where V is the plasma volume and ψ is the poloidal flux, are shown in Fig. 5 for both discharges. The uncertainty in s is ± 0.15 and increases slightly near $X = 1$. The shear profiles are the same for both plasmas and there was never a region of negative, or reverse, shear in either plasma. For both discharges at both times of interest, the shear increased smoothly from 0 at the magnetic axis until $X = 0.8$ where $s \approx 2$ and $q \approx 5$. After a small region of nearly constant shear, the shear increased rapidly to about 4 at the edge of the plasma. The shear profile remained unchanged to within the accuracy of the equilibrium reconstruction for the unspoiled supershot, except at the edge of the plasma. The change in shear caused by the gas puff for the spoiled supershot was also within the uncertainty of the reconstruction for $X < 0.8$. For $X > 0.8$, the change in shear is much larger and is due to the increase in $q(X=1)$ caused by the magnetic axis shift. The current profiles, which are not shown, have no substantial changes other than those consistent with the magnetic axis shift.

The measured plasma profiles may be summarized as follows: The gas puff caused changes in the q and shear profiles that were of the order of the uncertainty in the measurement and were similar to the evolution of the unspoiled discharge whereas the change in the ion thermal diffusivity profile was very large. Thus, within the uncertainty of the measurements, the enhanced confinement properties of the supershot regime do not depend on particular shapes or values of the q profile.

III. q Profile Variation

To assess the quantitative effect of varying the q-profile on supershot confinement, a set of supershot plasmas was prepared with different current ramps prior to the start of neutral beam injection, but with otherwise nominally identical conditions ($R = 2.61$ m, $B_t = 4.5$ T, $P_b = 17.5$ MW). The plasma current was increased from 1.0 to 1.4 MA, held flat at 1.4 MA, or else decreased from 2.0 to 1.4 MA prior to the start of auxiliary heating. The current ramp duration was 200 - 400 msec, and its timing was varied on successive discharges to change the degree of current penetration, with ramp end-times preceding the start of neutral injection by 0 - 1.5 sec. Figure 6 shows a comparison of "late" ramps, which ended just at the start of neutral injection, to a reference constant-current discharge. In Figs. 6 and 8, $\ell_i/2 \equiv \Lambda - \beta_{\text{Sup5}}(\text{dia}, \text{pol})$ has been used as a measure of the effective internal inductance. Therefore, the value of $\ell_i/2$ shown in 6(b) is only approximately correct because of the difference between $\beta_{\text{Sup5}}(\text{eq}, \text{pol})$ and $\beta_{\text{Sup5}}(\text{dia}, \text{pol})$.

Variations of the q profile produced either small or no changes in the peak τ_E attained in the discharge. The current ramp significantly altered the current density profile transiently as indicated by the change in $\ell_i/2$. The internal inductance, inferred from magnetics measurements 400 msec after beam injection began, varied from 0.5 (up-ramp) to 0.9 (down-ramp). The q profiles measured by MSE were very different as shown in Fig. 7. For the discharges shown in Fig. 6, the difference in τ_E at 4.4 sec was moderate in size, being ≈ 180 msec for the up-ramp versus ≈ 140 msec for the down-ramp. However, the peak value of τ_E occurred at different times after beam injection began. As shown in Fig. 6(d), the peak value of the energy confinement time was approximately the same for all three plasma current cases. At 4.4 sec (near the peak of the stored energy) there was a small trend of decreasing τ_E with increasing $\ell_i/2$.

The current ramps also caused a substantial, albeit transient, effect on the central ion temperature. Note that coherent MHD modes arose in the discharge with an I_p up-ramp starting at about 4.45 sec, which thenceforth spoiled the confinement, so the improvement in maximum stored energy, W_{tot} , was only about 12%.

Although there is a systematic correlation of decreasing τ_E near the time of peak stored energy [Fig. 8(a)] with increasing $\ell_i/2$, the correlation with edge recycling⁴ precludes us from concluding that

the q profile directly caused the improved confinement, since it could also result indirectly through the reduced recycling at lower $\ell_i/2$. In addition, the edge recycling during neutral injection appeared to vary systematically with the current ramp, with the better-performing plasmas having lower recycling. This is evident in both the time-dependent plots and in Fig. 8, which plots various quantities as a function of $\ell_i/2$ for the entire data set, including all of the different end-times of the current ramps. The edge emission from both H α and CII lines increases systematically with $\ell_i/2$, as does the edge electron density. The effect of current ramps on edge recycling was unexpected and is not consistent with simple recycling models which depend mostly on the power flux to the limiter and the degree of saturation of the limiter by deuterium. Also, the apparent decrease in τ_E is due to the choice of the sampling time, 400 msec after beam injection, when the plasma had approximately reached equilibrium and had approximately its peak stored energy.

The dependence of τ_E on $\ell_i/2$ in supershots differs from the behavior observed in L-mode¹⁵ and high poloidal beta³³ plasmas. In L-mode plasmas, χ_i and χ_e were found to be independent of $\ell_i/2$ in the region $r > a/2$, while $\tau_E/\tau_{E,L}$ increased with $\ell_i/2$ for low current-ramp rates. At higher ramp rates where q and the shear length, $L_s \equiv (q^2 R/r)(dq/dq)^{-1}$, are decorrelated, $\chi_{\text{Sup5}(tot,i)}$ was found to be proportional to L_s while $\chi_{\text{Sup5}(tot,e)}$ was independent of L_s .³⁴ In high β_{pol} plasmas, an increase in $\tau_E/\tau_{E,L}$ with $\ell_i/2$ was observed at the time of peaked stored energy.³³ A positive correlation of τ_E increasing with ℓ_i in L-mode and H-mode discharges was also observed in DIII-D.³⁵ Nevertheless, the data do establish a modest upper bound on the effect of the edge current density on supershot confinement. In particular, as shown in Fig. 8(b), the energy confinement times of all the current ramp discharges remain more than 2.1 times L-mode scaling. Thus, the supershot retains highly enhanced confinement, relative to L mode, for a large range of q profiles as inferred from the large range of $\ell_i/2$.

IV. Discussion

A correlation between the presence of coherent magnetohydrodynamic (MHD) modes and degradation of supershot performance has been observed by Chang *et al.*³⁶ A supershot typically reaches peak values of neutron emission, stored energy, and confinement time after a few hundred msec of beam injection. In most supershots, these values reach a steady-state value. However, in about 1/3 of

the supershot discharges, the stored energy decreases after the peak value has been reached by up to 30% with up to 60% degradation of the neutron emission rate. The performance deterioration depends upon the amplitude of the mode (or equivalently, the island width). So, while the ultimate performance of the supershot may be limited by MHD modes whose amplitude and effect may depend on the magnetic shear profile,³⁷ the supershot discharge still has greatly enhanced performance relative to an L-mode plasma even in the degraded state.

To improve stability of the supershot, discharges with high values of β_{pol} have been created by quickly decreasing the plasma current.³³ These plasmas have many of the same attributes as supershot plasmas and produce fusion powers similar to supershot plasmas but at 2/3 of the plasma current and are thus a good candidate for a reactor.³⁸ The increased stability is due to peaking of the current profile as represented by higher values of $l_i/2$. The energy confinement time has reached 4.5 times the L-mode scaling result, but has a relatively weak dependence on $l_i/2$.

It is also worth noting that the observed large changes in χ_i in the degraded supershot occurred much faster than any changes in the q profile. This implies that any transport model must be largely insensitive to the q profile. An alternate explanation of the data presented in Figs. 1 through 5 is that transport is extremely sensitive to the q profile. However, this cannot be true because rapidly changing the current (and drastically changing the q profile) does not change the enhanced confinement characteristics of the supershot.

The pellet-enhanced-performance (PEP) mode,³⁹ as developed on JET, shares many features of the supershot high confinement mode, but some significant differences exist. PEP mode discharges are characterized by peaked pressure profiles caused by a pellet-induced peaked density profile. The peaked pressure profile drives a large bootstrap current off-axis which may lead to an inverted q profile ($s < 0$).⁴⁰ Improved confinement may be caused by either the steep density gradient or by the inverted q profile.³⁹ The PEP mode discharges also have central temperatures of up to 15 keV and electron and ion temperatures about equal at central densities of 10^{20} m^{-3} or higher. While supershots also have high central densities and high temperatures, the electron and ion temperatures are not equal. Also, there is no indication of the q profile having a region of reversed shear, Figs. 4 and 7.

V. Critical-Electron-Temperature-Gradient Model

These discharges were used to test a proposed transport model, the critical-electron-temperature gradient, or RLW, model.^{11,22-25} This model assumes that anomalous transport is caused by turbulence in the magnetic field topology²³ that occurs when the spatial gradient of the electron temperature surpasses a critical value which is inversely proportional to q .¹¹ Functionally, the anomalous conductive heat losses are dependent upon the gradient of T_e , the ratio T_e/T_i , Z_{eff} , the electron density scale length, q , and the magnetic shear. The He-spoiled supershot provides a good test for this model because the temperatures are decreased, the gradients increased, and T_e/T_i increased by the gas puff as shown in Figs. 2 and 3, while the electron density scale length remains approximately constant and the q and shear profiles do not change at all, as shown in Figs. 4 and 5. Also, the condition of the carbon limiters was not changed.

The application of this model to the discharge is shown in Figs. 2 and 3. The model was run in a fully predictive fashion where both the T_e and T_i profiles were predicted from the measured equilibrium, Z_{eff} , and density profile. In Fig. 2, it can be seen that the RLW model does not match the profile before the gas puff. After the puff, the model and the measurements are in good agreement for $X > 0.4$, but differ by up to 30% for $X < 0.4$. The model fails to predict any change in the temperature profiles, even though $T_i(0)$ falls from 18 to 4 keV. The electron temperature profiles were also predicted by the model, Fig. 3. While the RLW model is within 1 keV of the measured T_e for $X > 0.4$ both before and after the puff, the model underestimates the central temperatures by up to 50%. The predicted changes in both temperature profiles are much less than that actually observed across the entire minor radius of the plasma.

VI. Conclusions

It has been shown in this paper that special shapes or values of the q profile are not responsible for the enhanced global confinement attributes of the supershot regime on TFTR. The confinement could change over a wide range while the current profile remained unchanged. Conversely, the q profile could be modified by a large amount with no large degradation in confinement. Therefore, the effect of the q profile on core energy confinement is too weak to be the dominant cause of improved confinement of supershot over L-mode plasmas.

The spoiled supershots were also used to test the predictive capabilities of the critical-electron-temperature-gradient model. It was found that this model could reproduce neither the values and shape of the temperature profiles nor the change in these profiles caused by the gas puff.

ACKNOWLEDGMENTS

Useful conversations with G. L. Schmidt and M. G. Bell and the support of K. M. Young, D. W. Johnson, and K. M. McGuire are gratefully acknowledged. This work was supported by the U. S. Department of Energy Contract No. DE-AC02-76-CHO-3073.

References

1. R. J. Goldston, *Plasma Phys. and Cont. Fusion* 26, 87 (1984).
2. J. D. Strachan, M. Bitter, A. T. Ramsey, M. C. Zarnstorff, V. Arunasalam, B. G. Bell, N. L. Bretz, R. Budny, C. E. Bush, S. L. Davis, H. F. Dylla, P. C. Efthimion, R. J. Fonck, E. Fredrickson, H. P. Furth, R. J. Goldston, L. R. Grisham, B. Grek, R. J. Hawryluk, W. W. Heidbrink, H. W. Hendel, K. W. Hill, H. Hsuan, K. P. Jaehnig, D. L. Jassby, F. Jobses, D. W. Johnson, L. C. Johnson, R. Kaita, J. Kamperschroer, R. J. Knize, T. Kozub, H. Kugel, B. LeBlanc, F. Levinton, P. H. L. Marche, D. M. Manos, D. K. Mansfield, K. McGuire, D. H. McNeill, D. M. Meade, S. S. Medley, W. Morris, D. Mueller, E. B. Nieschmidt, D. K. Owens, H. Park, J. Schivell, G. Schilling, G. L. Schmidt, S. D. Scott, S. Sesnic, J. C. Sinnis, F. J. Stauffer, B. C. Stratton, G. D. Tait, G. Taylor, H. H. Towner, M. Ulrickson, S. v. Goeler, R. Wieland, M. D. Williams, K.-L. Wong, S. Yoshikawa, K. M. Young, and S. J. Zweben, *Phys. Rev. Lett.* 58, 1004 (1987).
3. R. J. Hawryluk, V. Arunasalam, M. G. Bell, M. Bitter, W. R. Blanchard, N. L. Bretz, R. Budny, C. E. Bush, J. D. Callen, S. A. Cohen, S. K. Combs, S. L. Davis, D. L. Dimock, H. F. Dylla, P. C. Efthimion, L. C. Emerson, A. C. England, H. P. Eubank, R. J. Fonck, E. Fredrickson, H. P. Furth, G. Gammel, R. J. Goldston, B. Grek, L. R. Grisham, G. Hammett, W. W. Heidbrink, H. W. Hendel, K. W.

Hill, E. Hinnov, S. Hiroe, R. A. Hulse, H. Hsuan, K. P. Jaehrig, D. Jassby, F. C. Jobes, D. W. Johnson, L. C. Johnson, R. Kaita, J. Kamperschroer, S. M. Kaye, S. J. Kilpatrick, R. J. Knize, H. Kugel, P. H. LaMarche, B. LeBlanc, R. Little, C. H. Ma, D. M. Manos, D. K. Mansfield, M. P. McCarthy, R. T. McCann, D. C. McCune, K. McGuire, D. H. McNeill, D. M. Meade, S. S. Medley, D. R. Mikkelsen, S. L. Milora, W. Morris, D. Mueller, V. Mukhovatov, E. B. Nieschmidt, J. O'Rourke, D. K. Owens, H. Park, N. Pomphrey, B. Prichard, A. T. Ramsey, M. H. Redi, A. L. Roquemore, P. H. Rutherford, N. R. Sauthoff, G. Schilling, J. Schivell, G. L. Schmidt, S. D. Scott, S. Sesnic, J. C. Sinnis, F. J. Stauffer, B. C. Stratton, G. D. Tait, G. Taylor, J. R. Timberlake, H. H. Towner, M. Ulrickson, V. Vershkov, S. v. Goeler, F. Wagner, R. Wieland, J. B. Wilgen, M. Williams, K. L. Wong, S. Yoshikawa, R. Yoshino, K. M. Young, M. C. Zarnstorff, V. S. Zaveriaev, and S. J. Zweben, in *Plasma Physics and Controlled Nuclear Fusion Research, Proceedings of the 11th International Conference, Kyoto, 1986*, (International Atomic Energy Agency, Vienna, 1987), Vol. I, pp. 51.

4. J. D. Strachan, M. Bell, A. Janos, S. Kaye, S. Kilpatrick, D. Manos, D. Mansfield, D. Mueller, K. Owens, C. S. Pitcher, J. Snipes, and J. Timberlake, *J. Nucl. Materials* **196-198**, 28 (1992).

5. K. M. McGuire, H. Adler, P. Alling, C. Ancher, H. Anderson, J. L. Anderson, J. W. Anderson, V. Arunasalam, G. Ascione, D. Ashcroft, C. W. Barnes, G. Barnes, S. Batha, G. Bateman, M. Beer, M. G. Bell, R. Bell, M. Bitter, W. Blanchard, N. L. Bretz, R. Camp, M. Caorlin, Z. Chang, C. Z. Cheng, J. Chrzanowski, J. Collins, G. Coward, M. Cropper, D. S. Darrow, R. Daugert, J. DeLooper, W. Dorland, L. Dudek, H. Duong, R. Durst, P. C. Efthimion, D. Ernst, N. Fromm, G. Y. Fu, T. Fujita, H. P. Furth, V. Garzotto, C. Gentile, J. Gilbert, J. Gioia, N. Gorelenkov, B. Grek, L. R. Grisham, G. Hammett, G. R. Hanson, R. J. Hawryluk, D. L. Jassby, F. C. Jobes, D. W. Johnson, L. C. Johnson, M. Kalish, J. Kamperschroer, J. Kesner, H. Kugel, G. Labik, N. T. Lam, P. H. LaMarche, M. J. Loughlin, J. Machuzak, R. Majeski, D. K. Mansfield, E. S. Marmor, R. Marsala, A. Martin, G. Martin, E. Mazzucato, M. Mauel, M. P. McCarthy, J. McChesney, D. Mueller, M. Murakami, J. A. Murphy, A. Nagy, G. A. Navratil, R. Nazikian, R. Newman, M. Norris, T. O'Connor, M. Oldaker, J. Ongena, M. Osakabe, D. K. Owens, H. Park, W. Park, S. Pitcher, R. Pysher, A. L. Qualls, S. Raftopoulos, S. Ramakrishnan, A.

Ramsey, D. A. Rasmussen, M. H. Redi, G. Renda, G. Rewoldt, D. Roberts, G. Schilling, J. Schivell, G. L. Schmidt, R. Scillia, S. D. Scott, I. Semenov, T. Senko, S. Sesnic, R. Sissingh, C. H. Skinner, J. Snipes, J. Stencel, J. Stevens, W. Stodiek, W. Tighe, J. R. Timberlake, K. Tobita, H. H. Towner, M. Tuszewski, A. v. Halle, C. Vannoy, M. Viola, S. v. Goeler, D. Voorhees, R. T. Walters, R. Wester, R. White, R. Wieland, J. B. Wilgen, M. Yamada, S. Yoshikawa, K. M. Young, M. C. Zarnstorff, V. Zaveriev, and S. J. Zweben, *Phys. Plasmas* 2, 2176 (1995).

6. H. Weisen, H. Bergsaker, D. J. Campbell, S. K. Erents, L. C. J. M. d. Kock, G. M. McCracken, M. F. Stamp, D. D. R. Summers, P. R. Thomas, M. v. Hellermann, and J. Zhu, *Nucl. Fusion* 31, 2247 (1991).

7. K. H. Burrell, R. J. Groebner, T. S. Kurki-Suonio, T. N. Carlstrom, R. R. Dominguez, P. Gohl, R. A. Jong, H. Matsumoto, J. M. Lohr, T. W. Petrie, G. D. Porter, G. T. Sager, H. E. S. John, D. P. Schissel, S. M. Wolfe, and D.-D. R. Group, in *Plasma Physics and Controlled Nuclear Fusion Research 1990*, (International Atomic Energy Commission, Vienna, 1991), Vol. 1, pp. 123.

8. M. Kikuchi, M. Sato, Y. Koide, N. Asakura, Y. Kamada, T. Fukuda, S. Ishida, M. Mori, M. Shimada, and H. Ninomiya, 20th EPS Conference on Controlled Fusion and Plasma Physics, Lisboa (European Physical Society, Petit-Lancy, Switzerland, 1993), Part. 1, p. 179.

9. J. Ongena, A. M. Messiaen, G. V. Wassenhove, R. R. Weynants, P. Borgermans, P. Dumortier, F. Durodie, R. Koch, P. E. Vandenplas, R. V. Nieuwenhove, G. V. Oost, M. Vervier, H. Conrads, G. Bertschinger, H. G. Esser, H. Euringer, G. Fuchs, B. Giesen, B. Gorg, E. Graffmann, F. Hoenen, P. Huttemann, H. Keuer, M. Korten, H. R. Koslowski, W. Kohlhass, A. Kramer-Flecken, M. Lochter, G. Mank, A. Pospieszczyk, D. Rusbult, U. Samm, H. Schweer, S. Soltwisch, G. Telesca, R. Uhlemann, G. Waidmann, J. Winter, G. H. Wolf, and D. L. Hillis, in *Plasma Physics and Controlled Nuclear Fusion Research 1992*, (International Atomic Energy Commission, Vienna, 1993), Vol. 1, pp. 725.

10. S. D. Scott, C. W. Barnes, D. Ernst, J. Schivell, E. J. Synakowski, M. G. Bell, R. E. Bell, C. E. Bush, E. D. Fredrickson, B. Grek, K. W. Hill, A. Janos, D. L. Jassby, D. Johnson, D. K. Mansfield, D. K. Owens, H. Park, A. T. Ramsey, B. C. Stratton, M. Thompson, and M. C. Zarnstorff, U.S.-Japan Workshop on Ion Temperature Gradient-Driven Turbulent Transport, Austin, TX (AIP Press, 1994), Vol. 284, p. 19.
11. P.-H. Rebut, M. L. Watkins, D. J. Gambier, and D. Boucher, *Phys. Fluids B* **3**, 2209 (1991).
12. S. D. Scott, D. C. McCune, M. G. Bell, R. Bell, R. V. Budny, E. Fredrickson, B. Grek, K. W. Hill, D. Jassby, F. Jobs, D. W. Johnson, L. C. Johnson, D. K. Mansfield, H. K. Park, A. T. Ramsey, J. A. Snipes, B. E. Stratton, E. J. Synakowski, G. Taylor, H. H. Towner, and M. C. Zarnstorff, 19th European Physics Conference on Controlled Fusion and Plasma Physics, Innsbruck (European Physics Society, Petit-Lancy, Switzerland, 1992), Part. I, p. 39.
13. H. K. Park, M. G. Bell, W. M. Tang, G. Taylor, M. Yamada, R. V. Budny, D. C. McCune, and R. M. Weiland, *Nucl. Fusion* **34**, 1271 (1994).
14. M. C. Zarnstorff, R. J. Goldston, M. G. Bell, M. Bitter, C. Bush, R. J. Fonck, B. Grek, K. Hill, B. Howell, K. Jaehnig, D. Johnson, D. Mansfield, D. McCune, H. Park, A. Ramsey, J. Schivell, and G. Taylor, 16th European Physical Society Conference on Controlled Fusion and Plasma Heating, Venice (European Physics Society, Petit-Lancy, Switzerland, 1989), Part. I, p. 35.
15. M. C. Zarnstorff, C. W. Barnes, P. C. Efthimion, G. W. Hammett, W. Horton, R. A. Hulse, D. K. Mansfield, E. S. Marmor, K. McGuire, G. Rewoldt, B. C. Stratton, E. J. Synakowski, W. M. Tang, J. Terry, X. Q. Xu, M. G. Bell, M. Bitter, N. L. Bretz, R. Budny, C. E. Bush, R. J. Fonck, E. D. Fredrickson, H. P. Furth, R. J. Goldston, B. Grek, R. J. Hawryluk, K. W. Hill, H. H. and, D. W. Johnson, D. C. McCune, D. M. Meade, D. M. and, D. K. Owens, H. K. Park, A. T. Ramsey, M. N. Rosenbluth, J. Schivell, G. L. Schmidt, S. D. Scott, G. Taylor, and R. M. Wieland, in *Plasma Physics and Controlled*

Nuclear Fusion Research, Proceedings of the 13th International Conference, Washington, 1990, (International Atomic Energy Agency, Vienna, 1991), Vol. I, pp. 109.

16. M. C. Zarnstorff, N. L. Bretz, P. C. Efthimion, B. Grek, K. Hill, D. Johnson, D. Mansfield, D. McCune, D. K. Owens, H. Park, A. Ramsey, G. L. Schmidt, B. Stratton, E. Synakowski, and G. Taylor, 17th European Physical Society Conference on Controlled Fusion and Plasma Heating, Amsterdam (European Physics Society, Petit-Lancy, Switzerland, 1990), Part. I, p. 42.

17. M. Kotschenreuther, W. Dorland, M. A. Beer, and G. W. Hammett, *Phys. Plasmas* **2**, 2381 (1995).

18. G. Bateman, J. Weiland, H. Nordman, J. Kinsey, and C. Singer, *Physica Scripta* **51**, 597 (1995).

19. F. M. Levinton, R. J. Fonck, G. M. Gammel, R. Kaita, H. W. Kugel, E. T. Powell, and D. W. Roberts, *Phys. Rev. Lett.* **63**, 2060 (1989).

20. F. M. Levinton, *Rev. Sci. Instrum.* **63**, 5157 (1992).

21. F. M. Levinton, S. H. Batha, M. Yamada, and M. C. Zarnstorff, *Phys. Fluids B* **5**, 2554 (1993).

22. P. H. Rebut and M. Brusati, *Plasma Physics and Cont. Fusion* **28**, 113 (1986).

23. P. H. Rebut, P. P. Lallia, and M. L. Watkins, in *Plasma Physics and Controlled Nuclear Fusion Research, Proceedings of the 12th International Conference, Nice, 1988*, (International Atomic Energy Agency, Vienna, 1989), Vol. II, pp. 191.

24. P. H. Rebut, in *Plasma Physics and Controlled Nuclear Fusion Research, Proceedings of the 13th International Conference, Washington, 1990*, (International Atomic Energy Agency, Vienna, 1991), Vol. I, pp. 27.
25. A. Taroni, F. Tibone, B. Balet, D. Boucher, J. P. Christiansen, J. G. Cordey, G. C. Corrigan, D. F. Duchs, R. Giannella, A. Gondhalekar, N. Gottardi, G. M. D. Hogeweij, L. Lauro-Taroni, K. Lawson, M. Mattioli, D. Muir, J. O'Rourke, D. Pasini, P. H. Rebut, C. Sack, G. Sips, E. Springmann, T. E. Stringer, P. Stubberfield, K. Thomsen, M. L. Watkins, and H. Weisen, in *Plasma Physics and Controlled Nuclear Fusion Research, Proceedings of the 13th International Conference, Washington, 1990*, (International Atomic Energy Agency, Vienna, 1991), Vol. I, pp. 93.
26. M. Rosenbluth, J. Hogan, D. Boucher, A. Bondeson, P. Barabaschi, B. Coppi, L. Degtyarev, S. Haney, H. Goedbloed, T. C. Hender, H. Holties, G. Huysmanns, W. Kerner, J. Manickam, A. Martynov, S. Medvedev, D. Monticello, T. Ozeki, L. D. Pearlstein, F. Perkins, A. Pletzer, F. Porcelli, P.-H. Rebut, S. Tokuda, A. Turnbull, L. Villard, and J. Wesley, "ITER plasma modeling and MHD stability limits," in *Plasma Physics and Controlled Nuclear Fusion Research, Proceedings of the 15th International Conference, Seville, 1994*, (International Atomic Energy Agency, Vienna, in press).
27. A. T. Ramsey and D. M. Manos, *J. Nucl. Materials* **196-198**, 509 (1992).
28. R. J. Fonck, R. Howell, K. Jaehnig, L. Roquemore, G. Schilling, S. Scott, M. C. Zarnstorff, C. Bush, R. Goldston, H. Hsuan, D. Johnson, A. Ramsey, J. Schivell, and H. Towner, *Phys. Rev. Lett.* **63**, 520 (1989).
29. F. J. Stauffer, D. A. Boyd, R. C. Cutler, and M. P. McCarthy, *Rev. Sci. Instrum.* **56**, 925 (1985).
30. H. K. Park, *Rev. Sci. Instrum.* **61**, 2879 (1990).

31. S. P. Hirshman, D. K. Lee, F. M. Levinton, S. H. Batha, M. Okabayashi, and R. M. Wieland, *Phys. Plasmas* **1**, 2277 (1994).
32. S. H. Batha, F. M. Levinton, S. P. Hirshman, M. G. Bell, and R. M. Wieland, "Sensitivity of equilibrium profile reconstruction to motional-Stark-effect measurements," *submitted to Nuclear Fusion* (1995).
33. S. A. Sabbagh, R. A. Gross, M. E. Mauel, G. A. Navratil, M. G. Bell, R. Bell, M. Bitter, N. L. Bretz, R. V. Budny, C. E. Bush, M. S. Chance, P. C. Efthimion, E. D. Fredrickson, R. Hatcher, R. J. Hawryluk, S. P. Hirshman, A. C. Janos, S. C. Jardin, D. L. Jassby, J. Manickam, D. C. McCune, K. M. McGuire, S. S. Medley, D. Mueller, Y. Nagayama, D. K. Owens, M. Okabayashi, H. K. Park, A. T. Ramsey, B. C. Stratton, E. J. Synakowski, G. Taylor, R. M. Wieland, M. C. Zarnstorff, J. Kesner, E. S. Marmor, and J. L. Terry, *Phys. Fluids B* **3**, 2277 (1991).
34. M. C. Zarnstorff, G. Bateman, S. Batha, M. Beer, M. G. Bell, R. Bell, H. Biglari, M. Bitter, R. Boivin, N. L. Bretz, R. Budny, R. J. Hawryluk, W. Heidbrink, K. W. Hill, S. Hirshman, D. Hoffman, J. Hosea, M. Hughes, R. A. Hulse, A. Janos, F. Levinton, B. R. Majeski, D. M. Manos, D. K. Mansfield, E. S. Marmor, E. Mazzucato, D. K. Owens, H. Park, W. Park, S. Paul, F. Perkins, E. Perry, C. K. Phillips, M. Phillips, S. Pitcher, N. Pomphrey, D. Rasmussen, M. H. Redi, F. Rimini, G. Rewoldt, B. C. Stratton, J. D. Strachan, W. Stodiek, E. J. Synakowski, W. Tang, G. Taylor, J. Terry, M. Thompson, H. H. Towner, H. Tsui, M. Tuszewski, M. Ulrickson, S. v. Goeler, G. Wurden, K. L. Wong, P. Woskov, M. Yamada, K. M. Young, and S. J. Zweben, in *Plasma Physics and Controlled Nuclear Fusion Research 1992*, (International Atomic Energy Commission, Vienna, 1993), Vol. 1, pp. 111.
35. J. R. Ferron, L. L. Lao, and T. S. Taylor, 19th European Physics Conference on Controlled Fusion and Plasma Physics, Innsbruck (European Physics Society, Petit-Lancy, Switzerland, 1992), Part. I, p. 55.

36. Z. Chang, E. D. Fredrickson, J. D. Callen, K. M. McGuire, M. G. Bell, R. V. Budny, C. E. Bush, D. S. Darrow, A. C. Janos, L. C. Johnson, H. K. Park, S. D. Scott, J. D. Strachan, E. J. Synakowski, G. Taylor, R. M. Wieland, M. C. Zarnstorff, and S. J. Zweben, *Nucl. Fusion* **34**, 1309 (1994).
37. Z. Chang, J. D. Callen, E. D. Fredrickson, R. V. Budny, C. C. Hegna, K. M. McGuire, and M. C. Zarnstorff, *Phys. Rev. Lett.* **74**, 4663 (1995).
38. S. A. Sabbagh, M. E. Mael, G. A. Navratil, M. G. Bell, C. E. Bush, R. V. Budny, D. S. Darrow, E. D. Fredrickson, B. Grek, R. J. Hawryluk, H. W. Herrmann, A. Janos, D. W. Johnson, L. C. Johnson, B. LeBlanc, D. K. Mansfield, D. C. McCune, K. M. McGuire, D. Mueller, D. K. Owens, H. K. Park, A. T. Ramsey, C. Skinner, E. J. Synakowski, G. Taylor, R. M. Wieland, M. C. Zarnstorff, S. J. Zweben, S. H. Batha, F. M. Levinton, S. P. Hirshman, D. A. Spong, and J. Kesner, "Deuterium-tritium TFTR plasmas in the high poloidal beta regime," in *Plasma Physics and Controlled Nuclear Fusion Research, Proceedings of the 15th International Conference, Seville, 1994*, (International Atomic Energy Agency, Vienna, in press).
39. P. Smeulders, L. C. Appel, B. Balet, T. C. Hender, L. Lauro-Taroni, D. Stork, B. Wolle, S. Ali-Arshad, B. Alper, H. J. D. Blank, M. Bures, B. D. Esch, R. Gianella, R. Konig, P. Kupschus, K. Lawson, F. B. Marcus, M. Mattioli, H. W. Morsi, D. P. O'Brien, J. O'Rourke, G. J. Sadler, G. L. Schmidt, and P. M. Stubberfield, *Nucl. Fusion* **35**, 225 (1995).
40. M. Hugon, B. P. v. Milligan, P. Smeulders, L. C. Appel, D. V. Bartlett, D. Boucher, A. W. Edwards, L.-G. Eriksson, C. V. Gowers, T. C. Hender, G. Huysmans, J. J. Jacquiot, P. Kupschus, L. Porte, P. H. Rebut, D. F. H. Start, F. Tibone, B. J. D. Tubbing, M. L. Watkins, and W. Zwingmann, *Nucl. Fusion* **32**, 33 (1992).

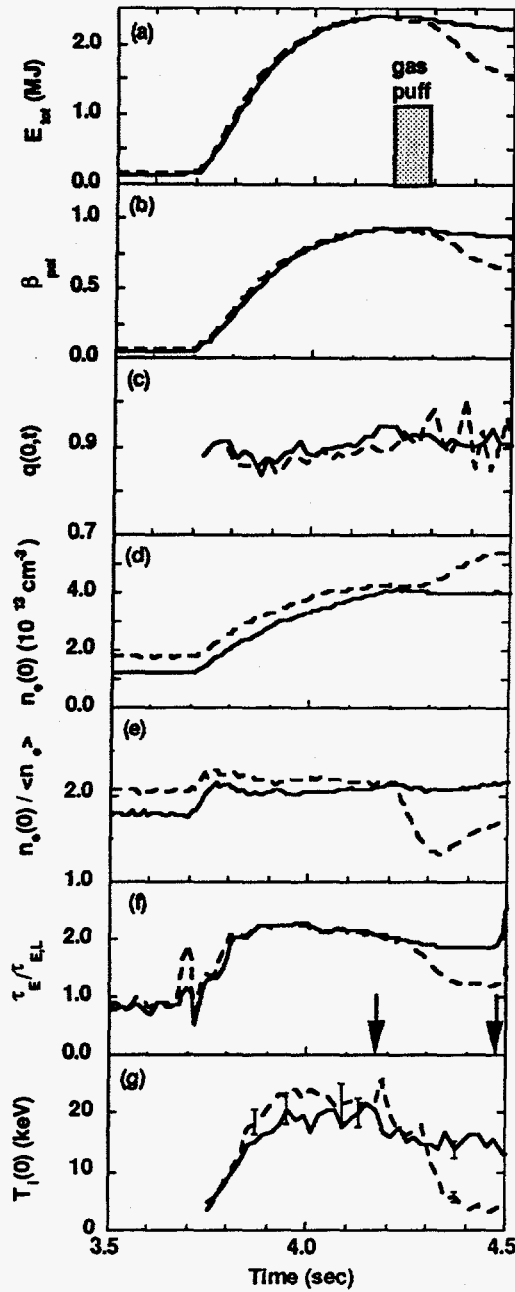


Fig. 1 The following plasma parameters are shown for a standard supershot (solid line) and a discharge spoiled to L-mode confinement (dashed line): (a) stored energy, (b) poloidal pressure β_{pol} , (c) central safety factor $q(0,t)$, (d) peak electron density $n_e(0)$, (e) electron density peakedness parameter, (f) energy confinement time enhancement factor $\tau_E/\tau_{E,L}$ where $\tau_{E,L}$ is the Goldston L-mode scaling, and (g) central ion temperature. The neutral beams injected 17.6 MW between 3.7 and 4.7 sec. The He gas puff was as shown on the spoiled discharge only. The arrows indicate when the profiles shown in the other figures were measured.

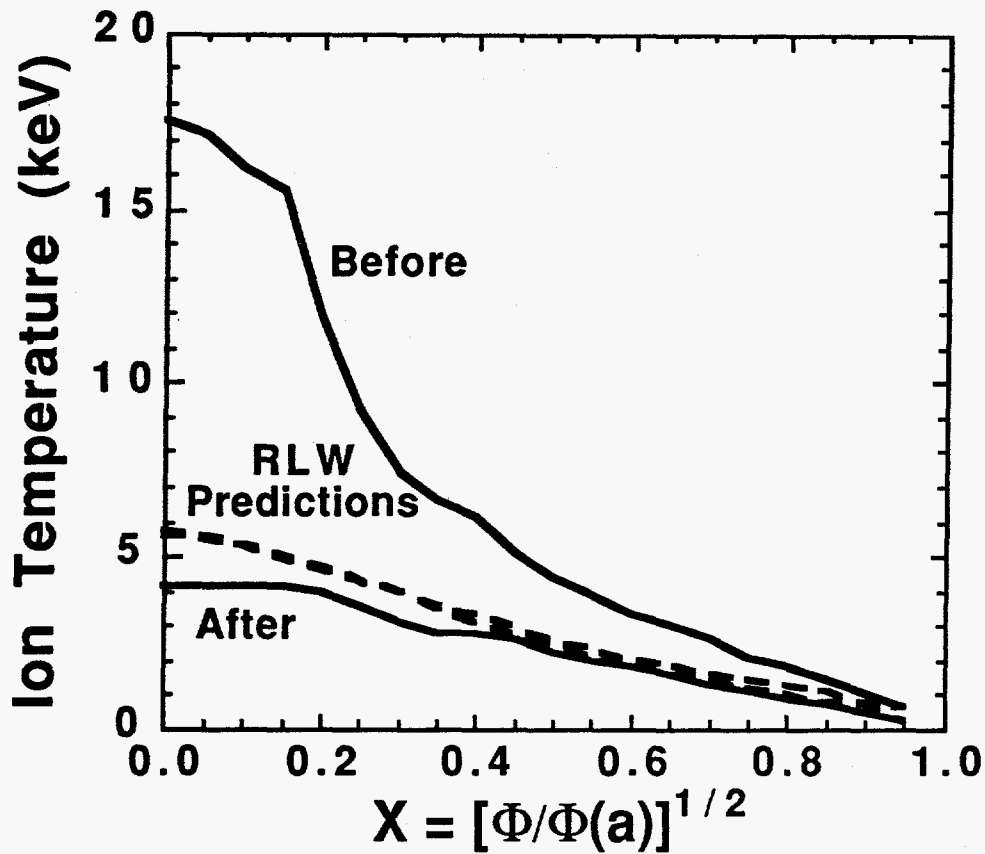


Fig. 2 Measured (solid line) and RLW-predicted (dashed line) ion temperature profiles from a spoiled supershot before (4.19 sec) and after (4.47 sec) the He gas puff. The RLW predictions are almost indistinguishable, but the edge temperature is predicted to decrease slightly. The abscissa is given as a function of the square root of the normalized toroidal flux Φ , where a is the minor radius of the plasma.

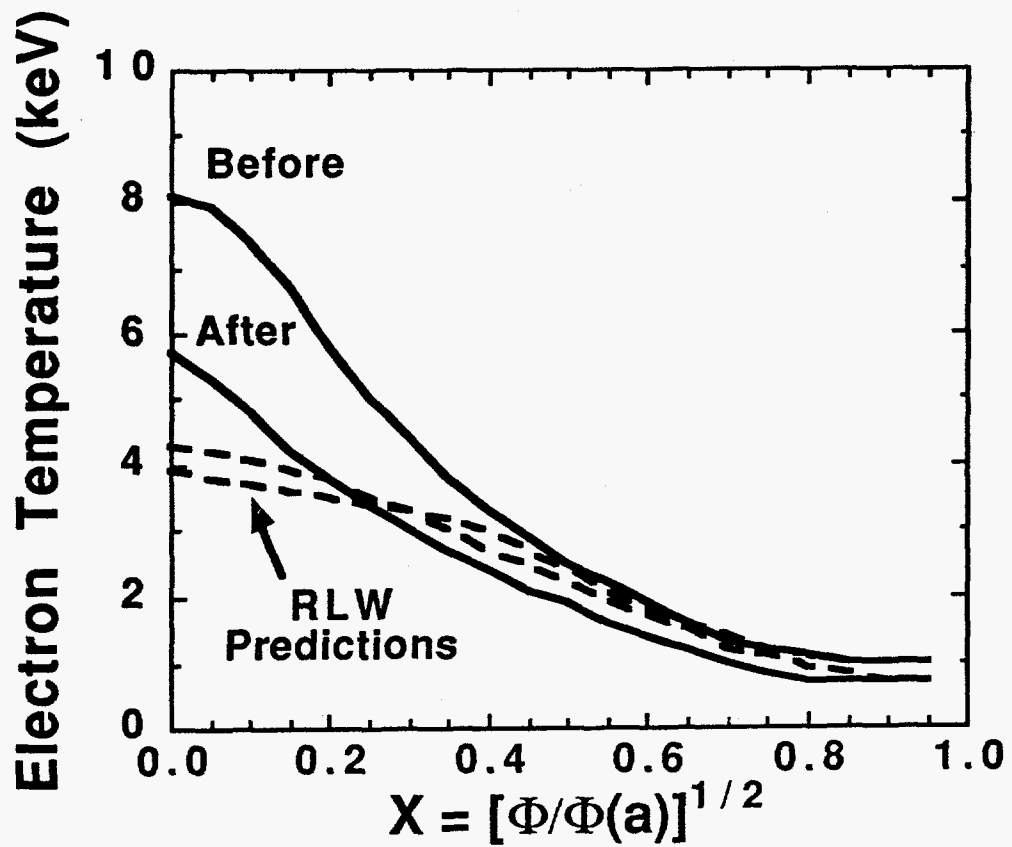


Fig. 3 Measured (solid line) and RLW-predicted (dashed line) electron temperature profiles from a spoiled supershot before (4.19 sec) and after (4.47 sec) the He gas puff. The RLW-prediction is that the central electron temperature increases while the edge ($X > 0.3$) decreases.

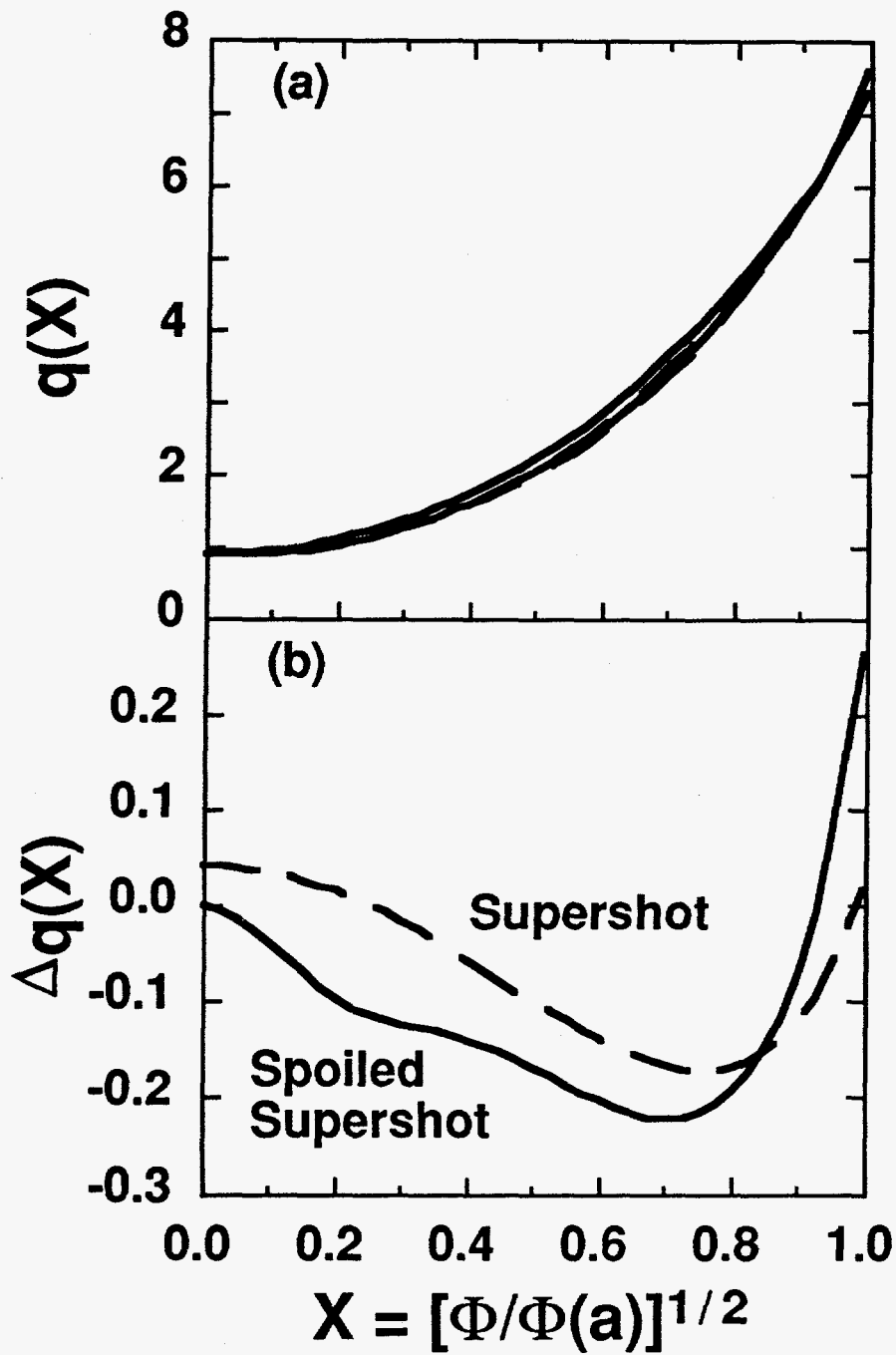


Fig. 4 The q profiles (a) before and after the He gas puff for the supershot (dashed lines) and spoiled supershot (solid lines). The difference in $q(X)$, $\Delta q(X) \equiv q(t=4.19) - q(t=4.47)$, is shown in (b). The uncertainty in $q(X)$ is less than 10% of $q(X)$.

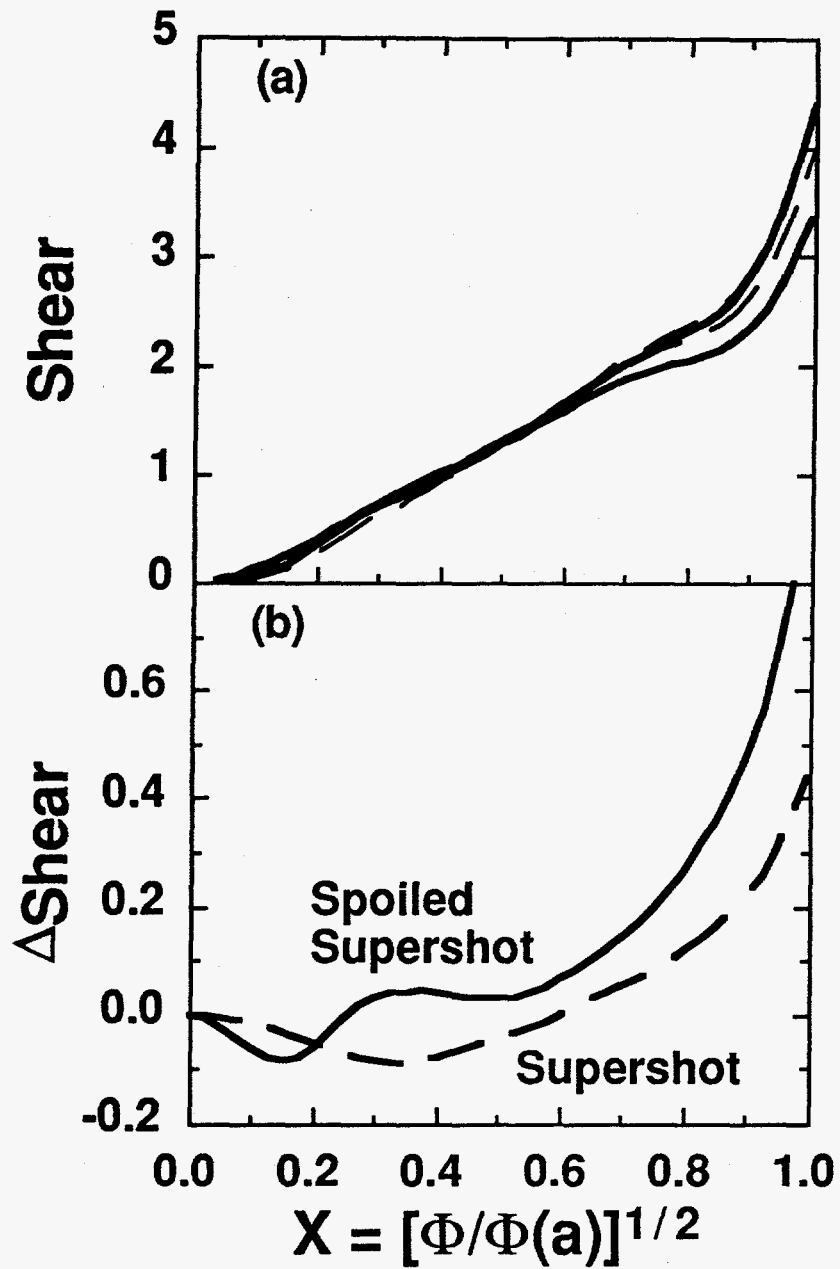


Fig. 5 The magnetic shear profiles (a) before and after the He gas puff for the supershot (dashed lines) and spoiled supershot (solid lines). The difference in Shear(X), $\Delta\text{Shear} \equiv \text{Shear}(t=4.19) - \text{Shear}(t=4.47)$, is shown in (b). The uncertainty in shear is less than ± 0.15 .

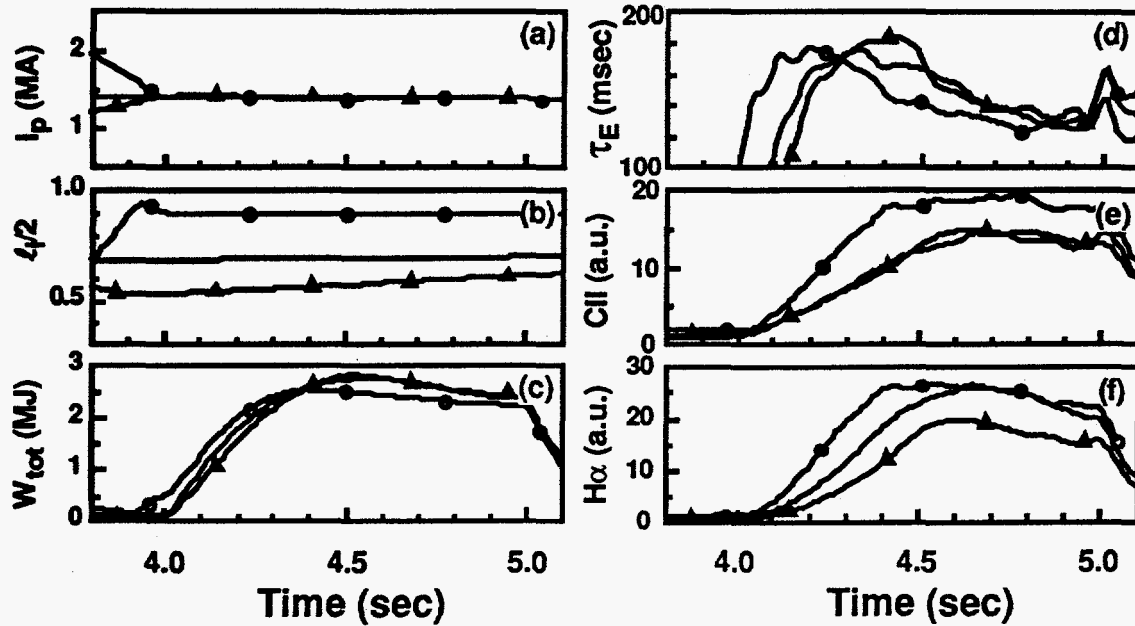


Fig. 6 Supershot performance for plasma current ramp-up (Δ), ramp-down (\circ), and constant-current (no symbol) discharges as a function of time. (a) Plasma current. (b) plasma inductance, $\ell/2$. (c) Stored energy, W_{tot} . (d) Global energy confinement time from equilibrium and diamagnetic magnetic diagnostics, including time-dependent corrections. (e) Edge H α emission. (f) Edge CII emission.

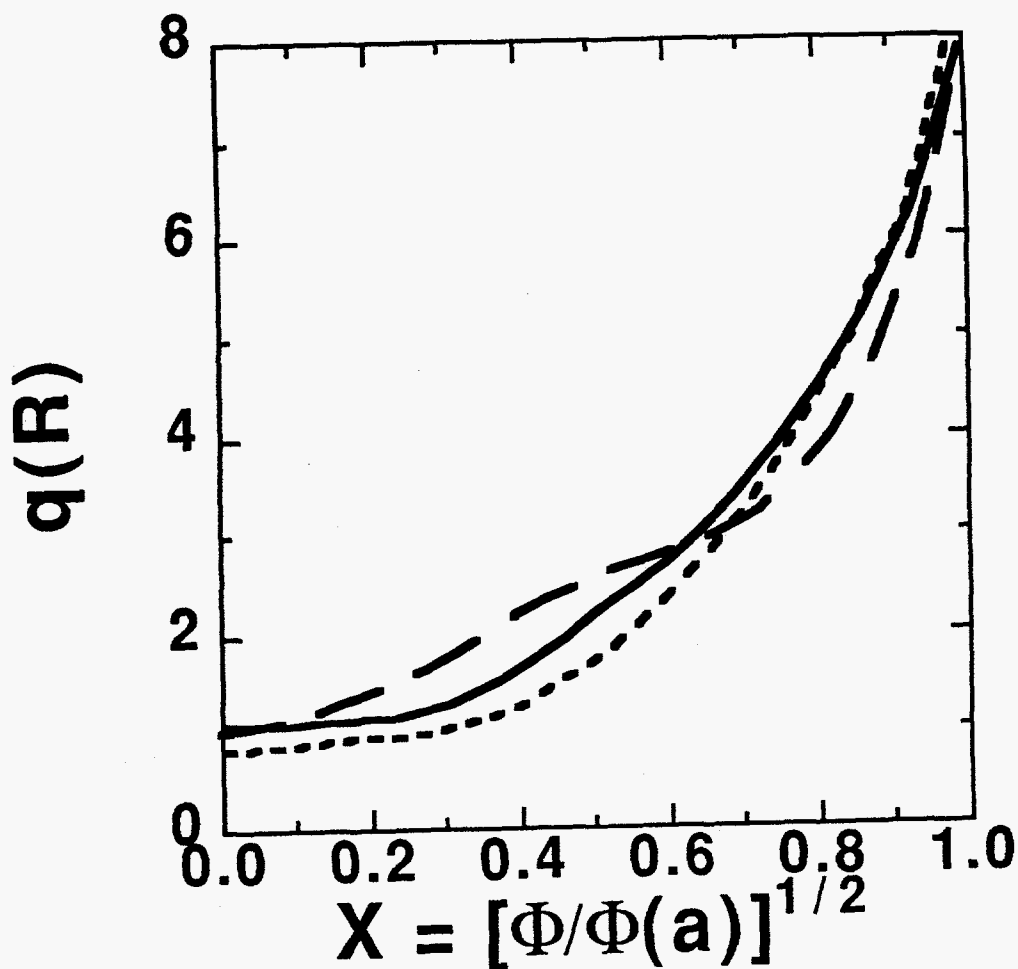


Fig. 7 q profile as measured by MSE for constant current (solid line), current ramp up (dashed line), and current ramp down (dotted line) supershot discharges of Fig. 6 at 4.5 sec.

DISCLAIMER

This report was prepared as an account of work sponsored by an agency of the United States Government. Neither the United States Government nor any agency thereof, nor any of their employees, makes any warranty, express or implied, or assumes any legal liability or responsibility for the accuracy, completeness, or usefulness of any information, apparatus, product, or process disclosed, or represents that its use would not infringe privately owned rights. Reference herein to any specific commercial product, process, or service by trade name, trademark, manufacturer, or otherwise does not necessarily constitute or imply its endorsement, recommendation, or favoring by the United States Government or any agency thereof. The views and opinions of authors expressed herein do not necessarily state or reflect those of the United States Government or any agency thereof.

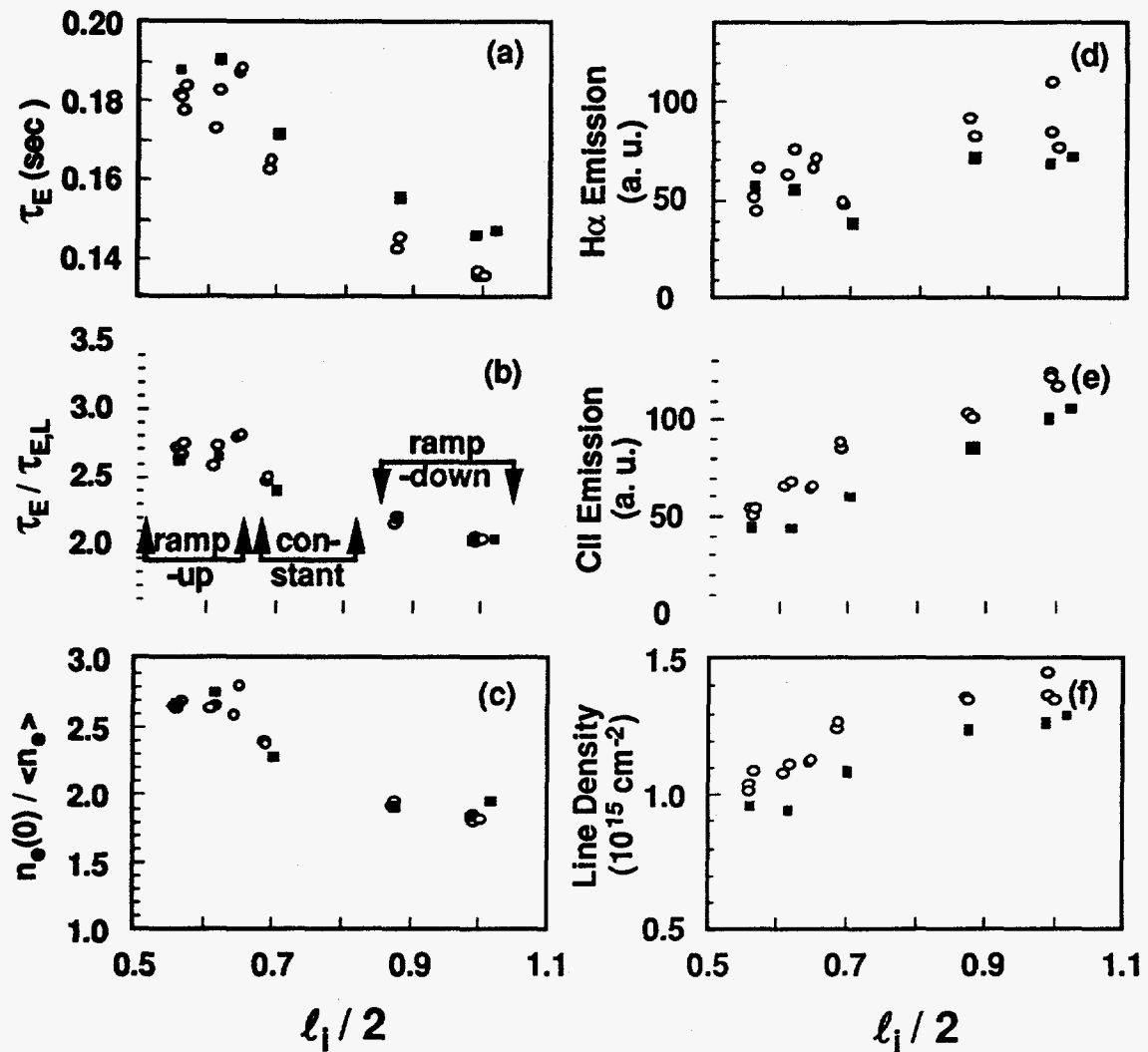


Fig. 8 Supershot performance after 400 msec of neutral-beam injection as a function of plasma inductance $l_i/2$. The data shown is for neutral-beam injection powers of 15.2 MW (■) and 17.5 MW (○). (a) Global energy confinement time from equilibrium and diamagnetic magnetic diagnostics, including time-dependent corrections. (b) Ratio of total stored energy to value predicted from L-mode scaling. (c) Peakedness of the electron density profile. (d) Edge H α emission. (e) Edge CII emission. (f) Vertical line integral electron density near the inner plasma edge, $R = 1.80$ m.